



Research article

Impact of subthalamic nucleus deep brain stimulation at different frequencies on neurogenesis in a rat model of Parkinson's disease

Zheng Wu^{a,d}, Zhiwei Ren^{a,d}, Runshi Gao^{a,d}, Ke Sun^b, Fangling Sun^c, Tingting Liu^c, Songyang Zheng^c, Wen Wang^{c,**}, Guojun Zhang^{b,*}

^a Department of Functional Neurosurgery, Xuanwu Hospital Capital Medical University, Beijing, China

^b Functional Neurosurgery Department, Beijing Children's Hospital, Capital Medical University, National Center for Children's Health, Beijing, China

^c Department of Experimental Animal Laboratory, Xuan-Wu Hospital of Capital Medical University, Beijing, China

^d Key Laboratory of Neurodegenerative Diseases (Capital Medical University), Ministry of Education, Beijing, China

ARTICLE INFO

Keywords:

Parkinson's disease
Subventricular zone
Deep brain stimulation
Subthalamic nucleus
Neurogenesis
Frequency

ABSTRACT

Neurogenesis, play a vital role in neuronal plasticity of adult mammalian brains, and its dysregulation is present in the pathophysiology of Parkinson's disease (PD). While subthalamic nucleus deep brain stimulation (STN-DBS) at various frequencies has been proven effective in alleviating PD symptoms, its influence on neurogenesis remains unclear. This study aimed to investigate the effects of 1-week electrical stimulation at frequencies of 60Hz, 130Hz, and 180Hz on neurogenesis in the subventricular zone (SVZ) of PD rats. A hemiparkinsonian rat model was established using 6-hydroxydopamine and categorized into six groups: control, PD, sham stimulation, 60Hz stimulation, 130Hz stimulation, and 180Hz stimulation. Motor function was assessed using the open field test and rotarod test after one week of STN-DBS at different frequencies. Tyrosine hydroxylase (TH) expression in brain tissue was analyzed via Western blot and immunohistochemistry. Immunofluorescence analysis was conducted to evaluate the expression of BrdU/Sox2, BrdU/GFAP, Ki67/GFAP, and BrdU/DCX in bilateral SVZ and the rostral migratory stream (RMS). Our findings revealed that high-frequency STN-DBS improved motor function. Specifically, stimulation at 130Hz increased dopaminergic neuron survival in the PD rat model, while significantly enhancing the proliferation of neural stem cells (NSCs) and neuroblasts in bilateral SVZ. Moreover, this stimulation effectively facilitated the generation of new NSCs in the ipsilateral RMS and triggered the emergence of fresh neuroblasts in bilateral RMS, with notable presence within the lesioned striatum. Conversely, electrical stimulation at 60Hz and 180Hz did not exhibit comparable effects. The observed promotion of neurogenesis in PD rats following STN-DBS provides valuable insights into the mechanistic basis of this therapeutic approach for PD.

1. Introduction

Parkinson's disease (PD) is a complex movement disorder that affects millions of people worldwide [1]. The clinical symptoms of

* Corresponding author. Functional Neurosurgery Department, Beijing Children's Hospital, Capital Medical University, National Center for Children's Health, No.56 Nanlishi Road, Xicheng District, Beijing 100045, China.

** Corresponding author. Department of Experimental Animal Laboratory, Xuanwu Hospital, Capital Medical University, No.45 Changchun Street, Xicheng District, Beijing, 10053, China.

E-mail addresses: lzwwang@163.com (W. Wang), zgjxwy@126.com (G. Zhang).

<https://doi.org/10.1016/j.heliyon.2024.e30730>

Received 23 April 2024; Accepted 2 May 2024

Available online 7 May 2024

2405-8440/© 2024 Published by Elsevier Ltd.

This is an open access article under the CC BY-NC-ND license

(<http://creativecommons.org/licenses/by-nc-nd/4.0/>).

PD include motor slowing, postural instability, rigidity, and resting tremor, which are caused by loss of dopamine neurons in the substantia nigra. The axons of these neurons project into the striatum, leading to a progressive and irreversible decrease in dopamine levels. Recent reports have demonstrated that alterations in neurotransmitter levels in PD patients affect adult neurogenesis in the subventricular zone (SVZ) [2,3]. Normally, adult neurogenesis in SVZ is that neural stem cells (NSCs) undergo in situ division and produce transit-amplifying progenitor cells. These cells transform into interneurons and radially migrate to the olfactory bulb (OB) by the rostral migratory stream (RMS) and differentiate into olfactory granule cells (GCs) and periglomerular cells, which integrate into

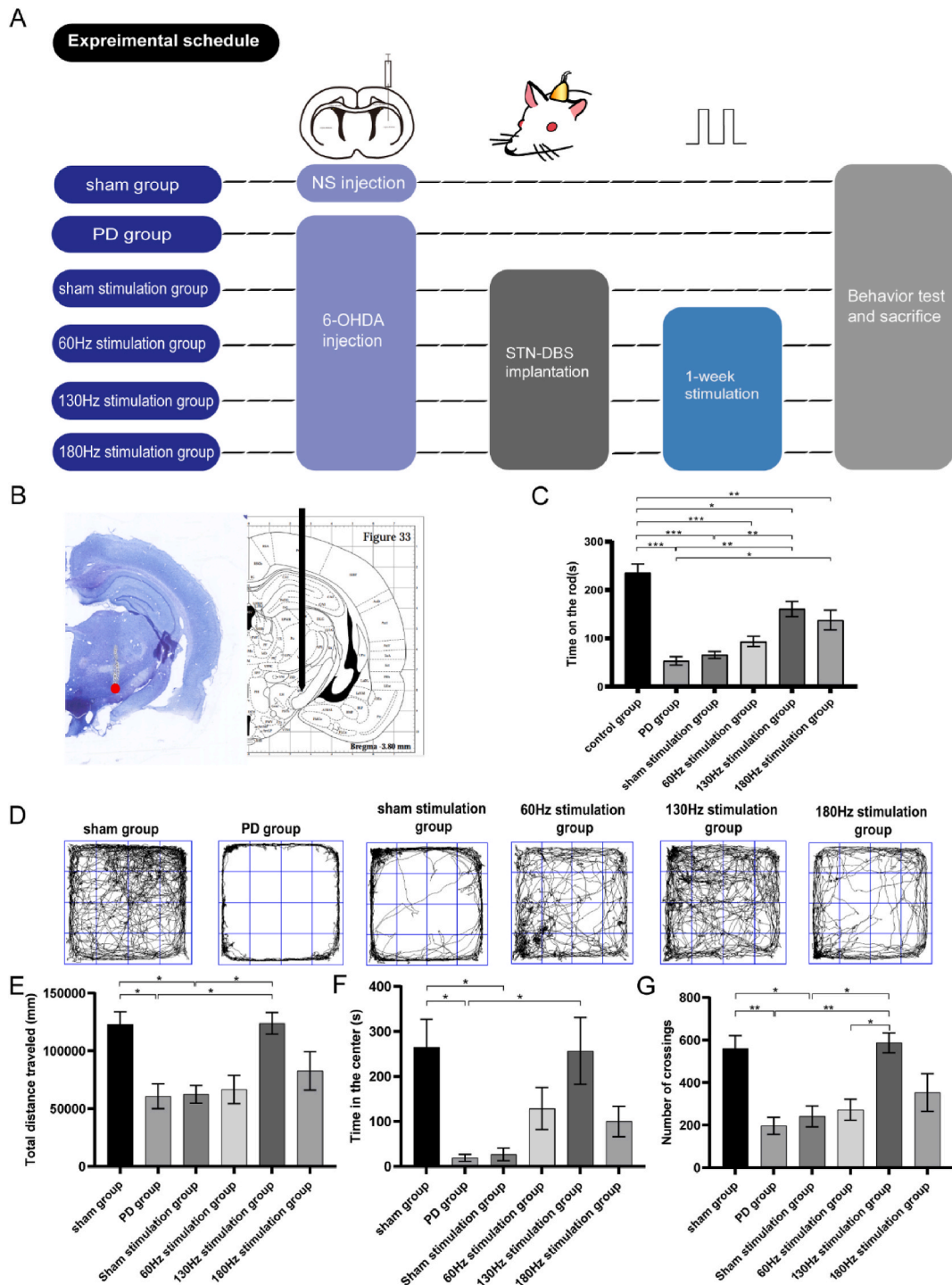


Fig. 1. STN-DBS improves motor behavior.

the neuronal circuitry [4,5]. However, it is generally accepted that the proliferation and differentiation of NSCs are influenced by changes of structures in many brain disorders, and new neurons can migrate to impaired regions to facilitate the restoration of neural function, thereby maintaining brain homeostasis [6].

Elly M. and colleagues have reported a subtle, albeit not statistically significant, decrease in the proliferation of NSCs in patients with PD [7]. Further investigations into the transcriptome and proteome of NSCs within the SVZ of PD patients revealed no notable changes in the activation state of these cells when compared to controls [8]. A significant decrease in EGFR⁺ cells within the SVZ of PD patients was observed in another study, suggesting a compromised proliferative capability of stem cells [9]. Animal models of PD have provided additional insights. In mice, the induction of PD through MPTP has been shown to lead to a significant increase in PH3-positive cells in the SVZ, contrasting with findings in human patients [7]. Furthermore, dopamine deficiency induced by MPTP in primate models of PD resulted in a decreased number of proliferating cells within the SVZ [10]. Aponso P. and colleagues demonstrated that after injecting 6-hydroxydopamine (6-OHDA) into the rat striatum, an increase in the proliferation of SVZ cells was observed in the first seven days, followed by a decline from days 14–28 [11]. These observations highlight the complex and variable response of NSCs to PD pathology. More detailed studies should be conducted to observe the neurological changes in humans and animals with PD, and explore the translational potential of NSC-based therapies in PD. Deep brain stimulation (DBS) targeting the subthalamic nucleus (STN) has proven to be an effective method for alleviating motor symptoms associated with PD. This treatment is typically employed when traditional pharmacological interventions fail to produce satisfactory results, particularly in advanced stages of the disease. People can effectively improve various clinical motor dysfunctions by manipulating the electrical parameters of neural stimulation. Among these parameters, frequency plays a crucial role in determining the efficacy of nerve electrical stimulation. High-frequency stimulation (130–185 Hz) of the STN-DBS has emerged as the most widely used treatment frequency for PD, demonstrating significant improvements in major motor functions. Conversely, low-frequency stimulation (60–80 Hz) has shown the ability to improve axial motor symptoms without negatively affecting limb tremors and freezing of gait [12–14]. At present, there are not many studies on the impact of STN-DBS on regulation of the proliferation and differentiation of NSCs in both the SVZ and the RMS. A post-mortem study has reported an increase in the number of NSCs within the ependymal layer adjacent to the hypothalamus in PD patients who underwent STN-DBS [15]. 130Hz STN-DBS in rats with 6-OHDA-induced PD has been shown to stimulate proliferation of BrdU⁺ cells in the SVZ [16]. In vitro cell culture studies have further demonstrated that electrical stimulation can enhance the proliferation, differentiation, migration, and integration of NSCs [17–19]. STN-DBS has the potential to modulate neuronal activity and regulate neurotransmitters [20–22]. Even so, it is not clear whether the different frequencies of STN-DBS simultaneously affect motor function and the proliferation and differentiation of NSCs in both the SVZ and the RMS. This knowledge gap hinders the advancement of clinical applications involving STN-DBS.

Therefore, our study focused on investigating the effects of unilateral STN-DBS at three different frequencies (60Hz, 130Hz, and 180Hz) in rats with PD induced by 6-OHDA. Through immunofluorescence staining, we aimed to explore the impact of these stimulation frequencies on the proliferation and differentiation of NSCs in the SVZ and RMS of the rats. This research endeavor aims to shed light on the influence of frequency-specific STN-DBS on neurogenesis in PD rats and provide supportive evidence for future investigations of the underlying molecular mechanisms of electrical stimulation.

2. Material and methods

2.1. Animals

The experimental procedure followed National Institute of Health Guide for the Care and Use of Laboratory. All animal protocols for this study were approved by the Animal Care and Use Committee of Xuanwu Hospital of Capital Medical University (Ethics Approval No. 20210417). Male Sprague-Dawley rats ($n = 60$, Five rats were not included due to electrode misplacement.) were used in this study and were provided with ad libitum access to food and water.

2.2. Experimental design

In the experimental design outlined in Fig. 1A, rats were stratified into six groups through random allocation. On day 1, an intracerebral injection of either 6-OHDA or normal saline was administered accordingly. Four weeks subsequent to this injection, STN-DBS devices were implanted into the brains of rats across all designated stimulation groups, inclusive of the sham stimulation cohort. Following a period of one week of electrical stimulation, motor function was assessed using behavioral tests. Subsequently, the animals' brains were harvested for further analysis.

2.3. 6-OHDA-induced PD model

Rats were anesthetized isofurane (5 % induction in 70 % nitrous oxide and 30 % oxygen and maintenance with 2 % isofurane) and placed on a stereotaxic frame. 10 μ g 6-OHDA in 2 μ L of saline with 0.02 % ascorbic acid was injected into right striatum at two sites: (anteroposterior [AP]: +1.6 mm, mediolateral [ML]: +2.4 mm, and dorsoventral [DV]: -4.2 mm; AP: -0.2 mm, ML: +2.6 mm, and DV: -7.0 mm). The rats in the control group were injected with normal saline at the same sites. The micro-injector was kept in place for an additional 5 min after the required volume was injected to ensure complete absorption of 6-OHDA. Rats were kept on a warm plate until they regained consciousness from anesthesia.

2.4. STN-DBS implantation

Rats were anesthetized with isofurane (5 % induction in 70 % nitrous oxide and 30 % oxygen and maintenance with 2 % isofurane), and secured on a stereotaxic frame (David Kopf, California, USA) at 4 weeks after 6-OHDA injection. The electrodes were placed after drilling and fixed by dental acrylic. The electrodes were fabricated from PFA-insulated tungsten (diameter 175 μm , California Fine Wire, Grover Beach, CA) with an 1 mm exposure (below 1 $\text{m}\Omega$). Stimulation parameters were as follows by a current-controlled stimulator (PlexStim, Plexon, Plano, TX): frequency, 60 Hz, 130 Hz, 180 Hz; intensity, 70–100 μA (It was determined by 90 % of the highest current which animals could be tolerated without side effects as previous report [23]); pulse width, 80 μs ; time: 24 h per day. The placement of electrodes in all rats was confirmed by using Nissl staining.

2.5. Behavioral testing

Apomorphine solution (Sigma-Aldrich: 0.5 mg apomorphine in 0.1 % ascorbate saline) at a dose of 0.5 mg/kg was subcutaneously injected, and rotations were monitored for 60 min after injection. Successful PD models were selected based on rotation rates exceeding 210 rotations per 30 min (seven turns per minute). In the rotarod test, rats were observed while remaining on a rotating rod starting from 0 to 40 revolutions per minute (r/min) for a duration of 5 min. The time spent on the rod was recorded for further analysis. Rats were placed in the center of an open field (100 cm \times 100 cm) in a dark room and allowed to move freely for 30 min. The apparatus was cleaned with 75 % ethanol and allowed to dry between tests. The tests were video-recorded and analyzed using Jiliang software (Shanghai Jiliang Software Technology Company, Shanghai, China).

2.6. Immunofluorescence and Immunohistochemical Analysis

BrdU (50 mg/kg; B5002, Sigma-Aldrich, St. Louis, MO, USA) was intraperitoneally injected twice daily for 3 days starting from the initiation of stimulation. Brain sections measuring 20 μm in thickness were obtained, and 6 every 10th section between bregma levels -0.60 and $+1.60$ mm was collected as the brain atlas. The first, middle and last sections were selected for immunohistochemical analysis. Subsequently, an additional 3 sections per brain, distinct from those used for immunohistochemical analysis, were randomly selected for immunofluorescence analysis. For BrdU staining, the sections were permeabilized with 0.1 M phosphate-buffered saline (PBS) containing 0.3 % Triton X-100 and incubated in 2 N HCl at 37 $^{\circ}\text{C}$ for 30 min, then washed by PBS three times before blocking in 3 % donkey serum (017-000-121, Jackson ImmunoResearch Laboratories, Philadelphia, USA). Samples were then incubated overnight at 4 $^{\circ}\text{C}$ with the following primary antibodies: rat anti-BrdU (1:200, ab6326, Abcam, Cambridge, MA, USA), goat anti-Sox2 (1:200, AF2018, R&D Systems, Minneapolis, MN, USA), mouse anti-GFAP (1:200, 3670S, CST, Danvers, MA, USA), rabbit anti-Doublecortin (DCX) (1:200, ab18723, Abcam, Cambridge, MA, USA), or rabbit anti-Ki67 (1:200, ab92391, Abcam, Cambridge, MA, USA). Appropriate Alexa Fluor 488- and Alexa Fluor 594-conjugated secondary antibodies were used to detect the primary antibodies (Alexa Fluor 488: A21206 and A32814, Alexa Fluor 594: A21209 and A21207, Life Technologies, Carlsbad, CA, USA). A mounting medium with 4,6-diamidino-2-phenylindole (DAPI) (Abcam) was used. The fluorescence signals were visualized using a fluorescence microscope (Nikon 80i, JPN). Three other sections of each animal were then treated with rabbit anti-Tyrosine Hydroxylase (TH) (1:200, ab112, Abcam, Cambridge, MA, USA) staining to evaluate level of TH⁺ neurites. Subsequently sections were incubated with a biotinylated goat anti-rabbit secondary antibody (PV-9001, Zhongshan Goldenbridge Biotechnology, Beijing, China) labeled with streptavidin-horseradish peroxidase at 37 $^{\circ}\text{C}$ for 30 min. The peroxidase activity was visualized with 3,3'-Diaminobenzidine (DAB) (ZLI-9018, Zhongshan Goldenbridge Biotechnology). The images were acquired using a light microscope and analyzed by image J. Immunofluorescence and Immunohistochemical Analysis were finally performed on samples obtained from a total of 30 rats.

2.7. Cell quantification

The acquisition parameters were kept consistent across different levels of magnification, utilizing a 10 \times objective for the SVZ and a 20 \times objective for the RMS. For the quantification of double-immunolabeled cells, including BrdU-positive/Sox2-positive, BrdU-positive/GFAP-positive, BrdU-positive/DCX-positive, and Ki67-positive/GFAP-positive, only cells lining the lateral ventricle wall were counted in the SVZ, and cells extending from the same SVZ to their terminal zones were counted in the RMS. The cell counts were then normalized to the number of cells per millimeter of SVZ or RMS length in each field of view. Additionally, BrdU-positive/DCX-positive cells in the lesioned striatum were quantified by counting cells per field of view adjacent to the SVZ.

2.8. Western blot analysis

The striatum of rats was harvested and washed with ice-cold NS solution, followed by lysis in a lysis buffer on ice for 30 min. Western blot analysis was finally performed on samples obtained from a total of 30 rats. After centrifugation at 12,000 $\times g$ for 30 min, protein concentration was determined using the BCA protein assay. Lysate protein (20 μg) was separated by SDS-PAGE on a 12 % gel and transferred to an NC membrane. After blocking with 5 % nonfat milk for 2 h, the membranes were incubated with primary antibodies overnight at 4 $^{\circ}\text{C}$: rabbit anti-TH (1:200, Abcam, Cambridge, MA, USA) and mouse anti- β -actin (TA-09, Zhongshanjinqiao, Inc., Beijing, China). Following primary antibody incubation, the membranes were then incubated with the respective secondary antibodies, either goat anti-mouse IgG or goat anti-rabbit IgG (Zhongshanjinqiao), for 1 h at room temperature. Protein bands were visualized using enhanced chemiluminescence (ECL) and analyzed using Image J.

2.9. Statistical analyses

Data are presented as mean \pm SEM. Differences between groups were evaluated using one-way analysis of variance (ANOVA) followed by a Scheffe post-hoc correction for multiple comparisons. All statistical analyses were performed using SPSS 21.0 software (SPSS, Inc., Chicago, IL, USA). A p-value <0.05 was considered significant for all tests. Pearson correlation was performed for cell counts and rotarod test. Pearson correlation matrix was generated by using excel Pearson function.

3. Result

1 STN-DBS improves motor function

To confirm the correct placement of the electrodes, Nissl staining was performed on brain sections and histological analysis revealed that the STN-DBS was accurately positioned (Fig. 1B). The rats in the PD group and sham stimulation group both exhibited a decreased time spent on the rod compared to the control group. However, rats subjected to 1-week 130 Hz electrical stimulation exhibited a significantly increased time spent on the rod compared to the PD group and the sham stimulation group. Additionally, the 180 Hz stimulation group also showed a significant increase in the time spent on the rod compared to the PD group. On the other hand, the 60 Hz electrical stimulation group did not show a significant improvement in the time spent on the rod (Fig. 1C). In the open field test, both the PD group and the sham stimulation group exhibited reduced locomotor activity and spent less time exploring the central area of the field compared to the control group. However, rats subjected to 1-week electrical stimulation showed a noticeable preference for exploring the central area (Fig. 1D). The rats in the 130 Hz stimulation group displayed a significant increase in movement distance compared to both the PD group and the sham stimulation group (Fig. 1E). Moreover, the 130 Hz stimulation group spent more time in the central area compared to the PD group (Fig. 1F). Additionally, the 130 Hz stimulation group exhibited a higher frequency of horizontal movements compared to both the PD group and the sham stimulation group (Fig. 1G). In summary, high-frequency electrical stimulation, particularly at 130 Hz, effectively improves motor impairments in rats.

A. Experimental design. Rats were randomly assigned to six groups. 6-OHDA or normal saline injection was performed on day 1; After four weeks, STN-DBS was implanted in the brain. After 1-week electrical stimulation, behavior test was used to evaluate motor function and animals were sacrificed. B. Trajectory of the DBS electrode. The optimal trajectory and target were determined by Nissl staining of brain sections (left side) with reference to the location of the STN (gray area) in the rat brain atlas (right side). The red dot indicated the electrode tip. C. Effect of STN-DBS on rotarod test performance after 1-week stimulation. D. Effect of STN-DBS on open field test performance. E. Effect of STN-DBS on total distance. F. Effect of STN-DBS on time in the center. G. Effect of STN-DBS on number of crossings. n = 5 rats per group, * $P < 0.05$; ** $P < 0.01$; *** $P < 0.001$.

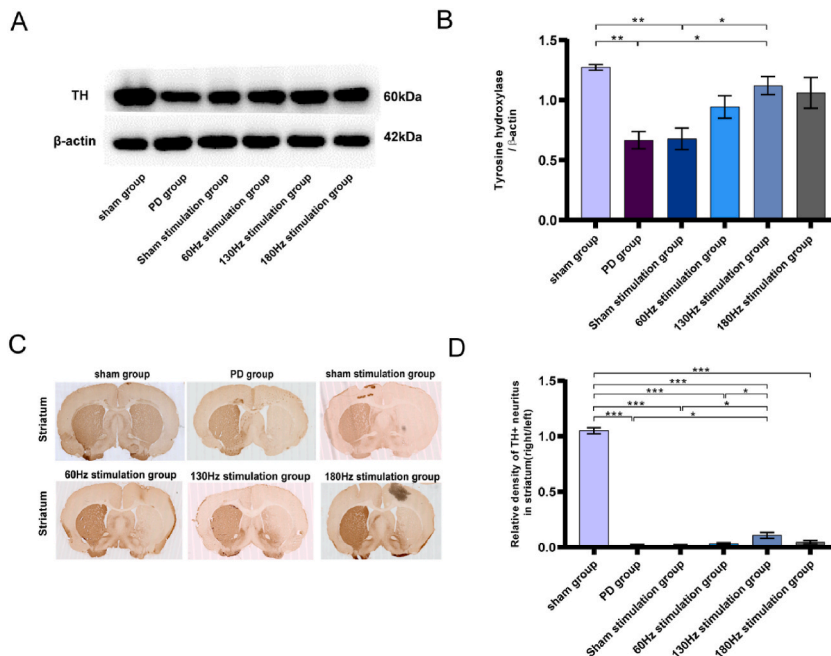


Fig. 2. STN-DBS rescues striatal TH⁺ neurons. A-B. TH expression in striatum was assessed by Western blot (n = 5). C-D. Quantitative analysis of TH⁺ neurites OD in the striatum. There were no differences in TH⁺ neurites OD between stimulation group and PD and sham stimulation groups (n = 5). * $P < 0.05$, ** $P < 0.01$; *** $P < 0.001$.

2 STN-DBS reduces dopaminergic neuron loss

The expression levels of tyrosine hydroxylase (TH) are commonly used to evaluate the loss of dopaminergic neurons [24]. Western blot analysis showed that both the PD group and the sham stimulation group exhibited a significant decrease in TH protein levels compared to the control group. However, rats subjected to 130 Hz electrical stimulation showed a notable restoration of TH protein

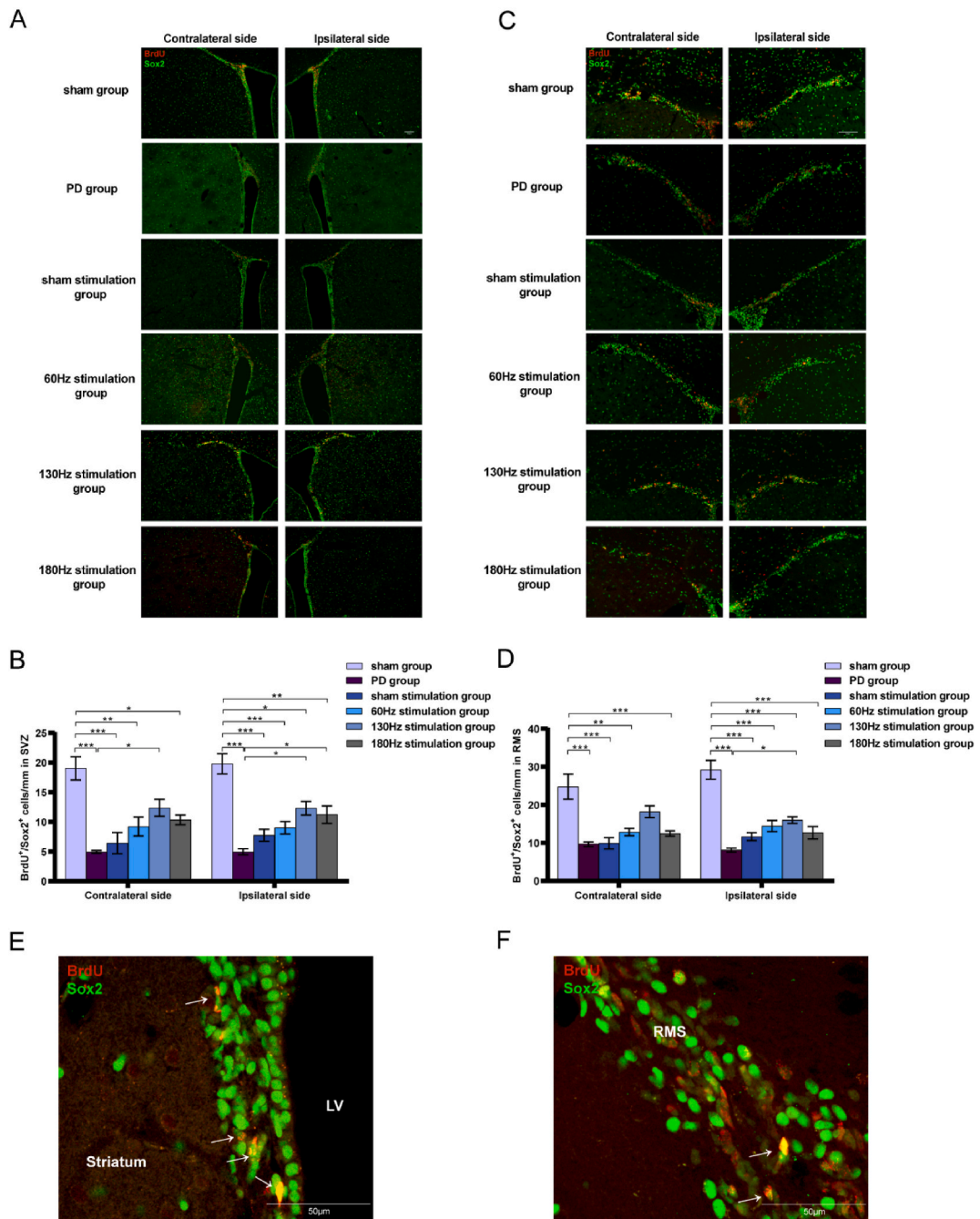


Fig. 3. Effect of STN-DBS on BrdU⁺/Sox2⁺ NSCs in the both sides of SVZ and RMS in PD rats. A. Double immunostaining of BrdU (red) with Sox2 (green) in the SVZ. B. 130Hz STN-DBS promoted Sox2⁺NSCs proliferation in the both sides of SVZ (n = 5). C. Double immunostaining of BrdU (red) with Sox2 (green) in the RMS. D. 130Hz STN-DBS promoted Sox2⁺ NSCs proliferation in the ipsilateral side of RMS (n = 5). E. High magnification showed double immunostaining of BrdU (red) with Sox2 (green) in the SVZ. Arrowheads indicate co-expression of BrdU and Sox2. F. High magnification showed double immunostaining of BrdU (red) with Sox2 (green) in the RMS. Arrowheads indicate co-expression of BrdU and Sox2. *P < 0.05, **P < 0.01; ***P < 0.001. LV, lateral ventricle.

levels in the lesioned striatum (Fig. 2A and B). Immunohistochemical staining further revealed a decrease in the relative density of TH nerve terminals in the striatum of the PD and sham stimulation groups. The 130 Hz stimulation group exhibited a significantly higher number of TH nerve terminals in the striatum compared to the PD and sham stimulation groups (Fig. 2C and D). There were no significant differences observed between the other frequency stimulation groups and the PD and sham stimulation groups. These findings suggest that 130 Hz STN-DBS has the potential to ameliorate the loss of dopamine neurons.

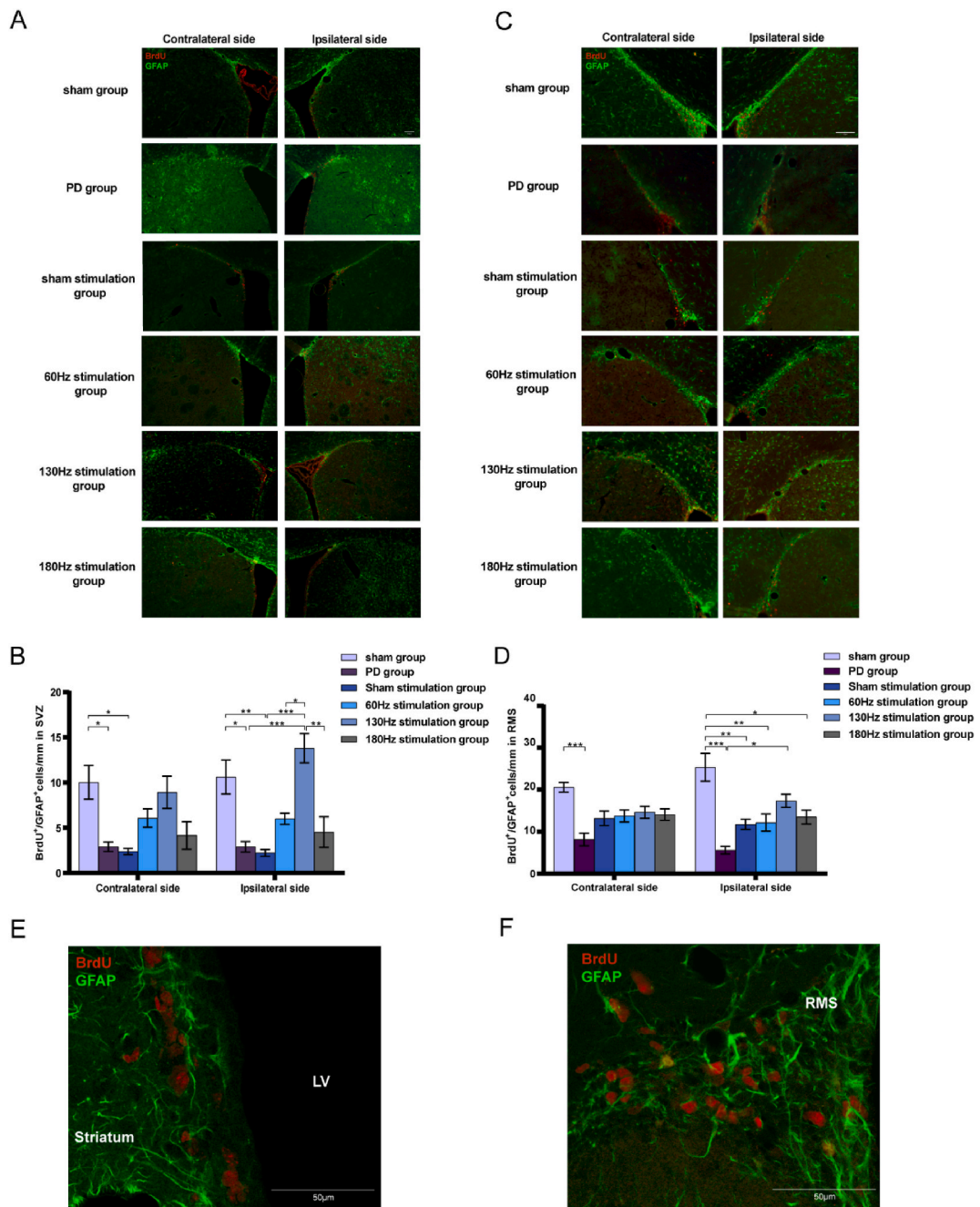


Fig. 4. Effect of STN-DBS on BrdU⁺/GFAP⁺ NSCs in the both sides of SVZ and RMS. A. Double immunostaining of BrdU (red) with GFAP (green) in the SVZ of rats. B. 130Hz STN-DBS promotes GFAP⁺ NSCs proliferation in the ipsilateral side of SVZ (n = 5). C. Double immunostaining of BrdU (red) with GFAP (green) in the RMS of rats. D. 130Hz STN-DBS promotes GFAP⁺ NSCs proliferation in the ipsilateral side of RMS (n = 5). E. High magnification showed double immunostaining of BrdU (red) with GFAP (green) in the SVZ. Arrowheads indicate co-expression of BrdU and GFAP. F. High magnification showed double immunostaining of BrdU (red) with GFAP (green) in the RMS. Arrowheads indicate co-expression of BrdU and GFAP. *P < 0.05, **P < 0.01; ***P < 0.001. LV, lateral ventricle.

3 STN-DBS promotes neurogenesis

3.1 STN-DBS promotes proliferation of NSCs

To investigate the effects of electrical stimulation at different frequencies on neurogenesis, we examined the proliferation of NSCs

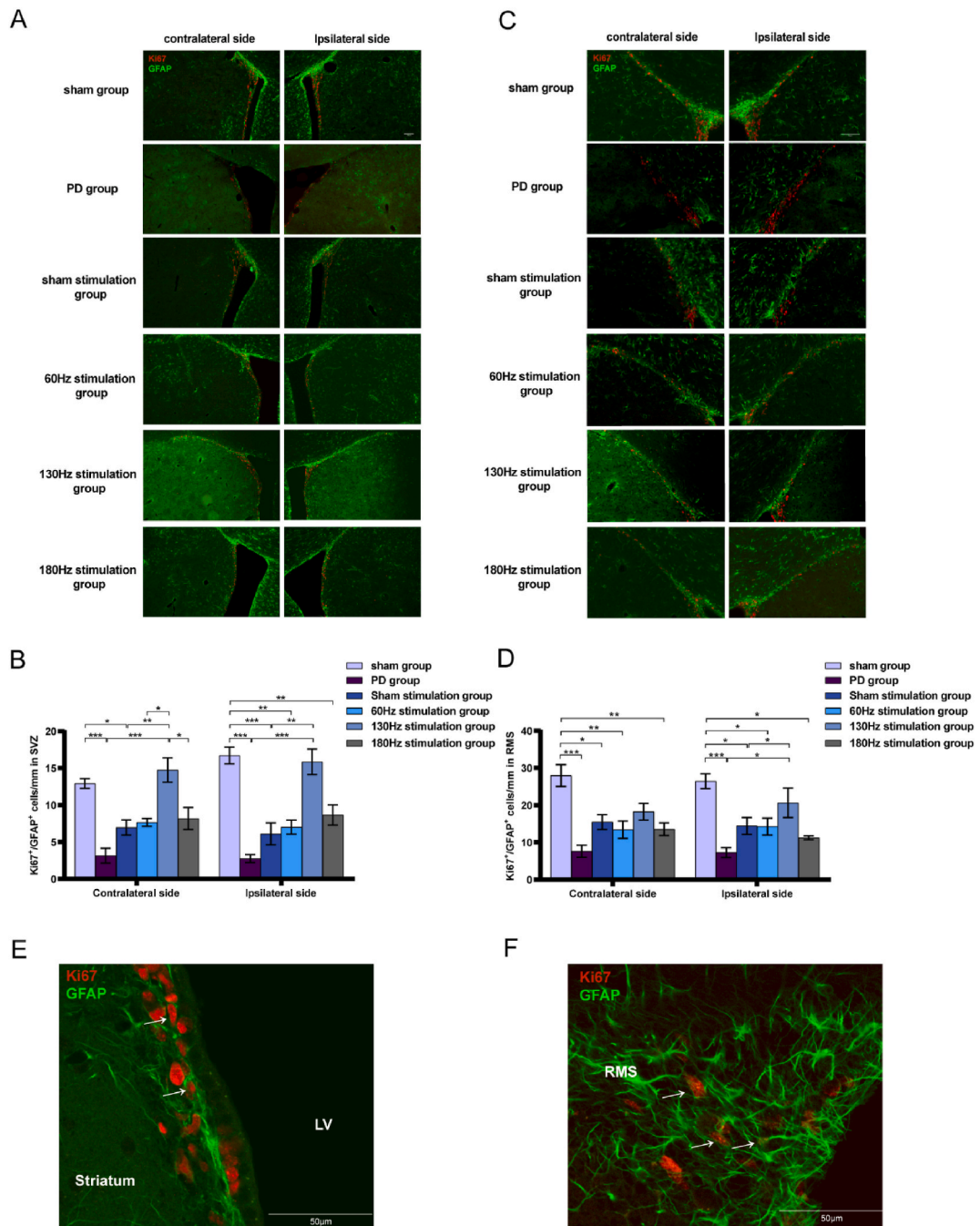


Fig. 5. Effect of STN-DBS on Ki67⁺/GFAP⁺ NSCs in the both sides of SVZ and RMS. A. Double immunostaining of Ki67 (red) with GFAP (green) in the SVZ of rats. B. 130Hz STN-DBS promotes precursor proliferation in the both sides of SVZ (n = 5). C. Double immunostaining of Ki67 (red) with GFAP (green) in the RMS of rats. D. 130Hz STN-DBS promotes neural precursor proliferation in the ipsilateral side of RMS (n = 5). E. High magnification showed double immunostaining of Ki67 (red) with GFAP (green) in the SVZ. Arrowheads indicate co-expression of Ki67 and GFAP. F. High magnification showed double immunostaining of Ki67 (red) with GFAP (green) in the RMS. Arrowheads indicate co-expression of Ki67 and GFAP. *P < 0.05, **P < 0.01; ***P < 0.001. LV, lateral ventricle.

in the SVZ and RMS. We used BrdU, a thymidine analogue, to label actively dividing cells during the S phase of the cell cycle and detect newly generated cells [25]. Sox2 is an NSC marker that actively regulates self-renewal of NSCs (Fig. 3A). Immunofluorescence analysis showed a significant decrease in the presence of BrdU⁺/Sox2⁺ cells in both the SVZ and RMS of the PD group and the sham stimulation group compared to the control group after 6-OHDA induction. However, compared to the PD group, both the 130 Hz and 180 Hz

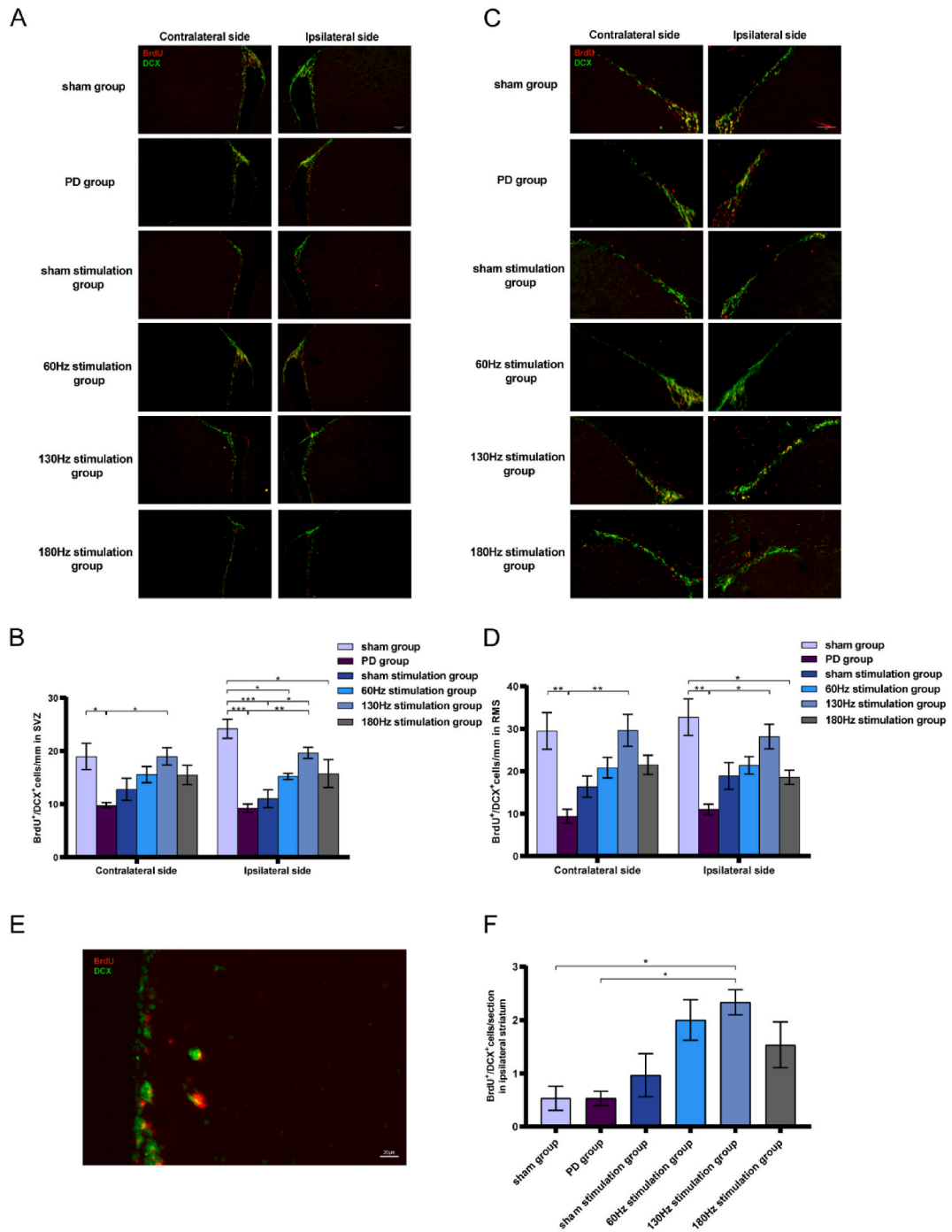


Fig. 6. Effect of STN-DBS on neuroblasts proliferation in the both sides of SVZ and RMS. A. Double immunostaining of BrdU (red) with DCX (green) in the SVZ of rats. B. 130Hz STN-DBS promotes neuroblasts proliferation in the both sides of SVZ (n = 5). C. Double immunostaining of BrdU (red) with DCX (green) in the RMS of rats. D. 130Hz STN-DBS promotes neuroblasts proliferation in the both sides of RMS (n = 5). E. Double immunostaining of BrdU (red) with DCX (green) in the ipsilateral striatum next to SVZ. F. 130Hz STN-DBS promotes generation of newly born neuroblasts in the lesioned striatum next to SVZ (n = 5). *P < 0.05, **P < 0.01; ***P < 0.001.

stimulation groups significantly increased the number of BrdU⁺/Sox2⁺ cells in the ipsilateral SVZ. Moreover, the contralateral SVZ of the 130 Hz stimulation group had a higher number of BrdU⁺/Sox2⁺ cells compared to the PD group (Fig. 3B). In the RMS, the 130 Hz stimulation effectively restored the decreased number of BrdU⁺/Sox2⁺ cells on the affected side (Fig. 3C and D). These findings indicate that 130 Hz stimulation promotes NSC proliferation in the SVZ and RMS of PD rats, while low-frequency stimulation does not have a similar effect on proliferation (Fig. 3B–D). High magnification investigations revealed the overlapping staining for BrdU and Sox2 (Fig. 3E and F). Furthermore, the number of BrdU⁺/Sox2⁺ cells in both sides of SVZ and RMS correlates well with the time on rods in rotarod results respectively (Supplemental Fig. 1).

We also examined the proliferation of NSCs in the SVZ and RMS using BrdU/GFAP staining (Fig. 4A). The results showed a significant decrease in the number of BrdU⁺/GFAP⁺ cells in the bilateral SVZ of the PD group and the sham stimulation group compared to the control group. However, rats receiving 130 Hz electrical stimulation exhibited a noteworthy increase in the number of BrdU⁺/GFAP⁺ cells in the ipsilateral SVZ (Fig. 4B). In the RMS, a reduced number of BrdU⁺/GFAP⁺ cells were observed bilaterally in the PD group compared to the control group. Nevertheless, unilateral 130 Hz electrical stimulation effectively increased the population of BrdU⁺/GFAP⁺ cells on the ipsilateral side of the RMS. In contrast, low-frequency and high-frequency (180 Hz) electrical stimulation did not have a significant impact on cell proliferation (Fig. 4B–D). High magnification investigations revealed the staining for BrdU⁺/GFAP⁺ cells (Fig. 4E and F). And cell counts of BrdU⁺/GFAP⁺ cells observed in both sides of SVZ and RMS were found to have a positive and significant linear correlation with the time spent on the rods in the rotarod test results (Supplemental Fig. 2).

Ki67 positivity signifies cells in an active proliferative state. Dual staining for Ki67 and GFAP can be employed to visualize the proliferation of SVZ NSCs (Fig. 5A). Compared to the control group, both the PD group and the sham stimulation group exhibited a significant bilateral reduction in the number of Ki67⁺/GFAP⁺ cells in the SVZ. However, administration of 130Hz electrical stimulation notably restored Ki67⁺/GFAP⁺ cell proliferation in the bilateral SVZ (Fig. 5B). In the PD group, there was a significant decline in Ki67⁺/GFAP⁺ cell count in the bilateral SVZ. Remarkably, 130Hz electrical stimulation specifically facilitated the proliferation of Ki67⁺/GFAP⁺ cells in the affected side of the RMS (Fig. 5C and D). Conversely, neither the low-frequency stimulation group nor the 180Hz stimulation group displayed any substantial increase in proliferation in both the SVZ and the RMS (Fig. 5B–D). High magnification investigations revealed the staining for Ki67⁺/GFAP⁺ cells (Fig. 5E and F). Furthermore, cell counts of Ki67⁺/GFAP⁺ cells observed in both sides of SVZ and RMS were found to have a positive and significant linear correlation with the time spent on the rods in the rotarod test results (Supplemental Fig. 3).

Through the cumulative findings of this study, we have established a strong evidentiary basis for the efficacy of 130Hz electrical stimulation in promoting the proliferation of NSCs, which significantly enhances neurogenesis. This enhancement in neurogenesis is closely associated with improved motor recovery in PD, underlining the therapeutic potential of electrical stimulation interventions.

2.2 STN-DBS promotes proliferation of neuroblasts

DCX, a well-established marker for neuroblasts, has traditionally been associated with the neuronal lineage of differentiated cells

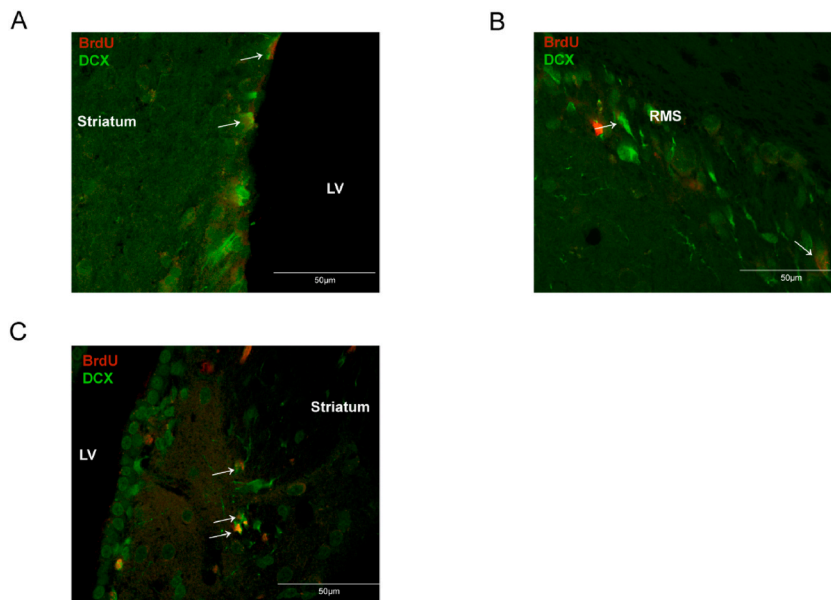


Fig. 7. High magnification investigations of BrdU⁺/DCX⁺ cells. A. High magnification showed double immunostaining of BrdU (red) with DCX (green) in the SVZ. Arrowheads indicate co-expression of BrdU and DCX. B. High magnification showed double immunostaining of BrdU (red) with DCX (green) in the RMS. Arrowheads indicate co-expression of BrdU and DCX. C. High magnification showed double immunostaining of BrdU (red) with DCX (green) in the striatum. Arrowheads indicate co-expression of BrdU and DCX. LV, lateral ventricle.

and integrated into local interneurons [26]. In this study, we performed BrdU/DCX double staining to examine the proliferation of neuroblasts in each experimental group following electrical stimulation (Fig. 6A). The results revealed a significant decrease in the quantity of BrdU⁺/DCX⁺ cells within the ipsilateral SVZ of both the PD group and the sham stimulation group, as well as in the contralateral SVZ of the PD group, compared to the control group. The implementation of 130Hz electrical stimulation yielded a pronounced augmentation in the populace of BrdU⁺/DCX⁺ cells within the bilateral SVZ. The application of 130Hz electrical stimulation resulted in a marked increase in BrdU⁺/DCX⁺ cells in the bilateral SVZ when compared to the PD group and unilateral side of SVZ in the sham stimulation group (Fig. 6B). Furthermore, a considerable decrease in the number of BrdU⁺/DCX⁺ cells in the bilateral RMS was observed in the PD group as compared to the control group. Interestingly, unilateral 130Hz electrical stimulation led to an elevated number of BrdU⁺/DCX⁺ cells on both sides of the RMS. On the other hand, neither the low-frequency stimulation group nor the high frequency (180Hz) stimulation group exhibited a significant increase in the SVZ and RMS (Fig. 6C and D). Intriguingly, we also detected the presence of BrdU⁺/DCX⁺ cells in the striatum adjacent to the SVZ. The number of such cells in the 130Hz electrical stimulation group was markedly higher than that observed in both the PD and control groups (Fig. 6E and F). High magnification investigations revealed the overlapping staining for BrdU and DCX (Fig. 7A–C). And cell counts of BrdU⁺/DCX⁺ cells observed in both sides of SVZ and RMS were found to have a positive and significant linear correlation with the time spent on the rods in the rotarod test results (Supplemental Fig. 4). However, the number of BrdU⁺/DCX⁺ cells in the striatum cannot be linear correlated significantly (Supplemental Fig. 5A). Interestingly, when data of the control group are excluded from the analysis, a significant correlation emerges between the number of BrdU⁺/DCX⁺ cells in the striatum and the rotarod test results (Supplemental Fig. 5B). These findings suggest that 130Hz electrical stimulation promotes the generation of neuroblasts that may potentially migrate to the striatum for reparative processes, which may contribute to motor recovery in PD.

4. Discussion

This study examines how neurogenesis in the SVZ and RMS is altered in rats with PD following one week of STN-DBS at different frequencies. The results indicate that STN-DBS at a frequency of 130Hz improved motor deficits, protected against dopaminergic neuron loss, and promoted the proliferation and differentiation of NSCs in the SVZ and RMS of rats injected with 6-OHDA.

The administration of 6-OHDA, a commonly used toxin in PD animal models, induces oxidative stress and inhibition of the mitochondrial respiratory chain by generation of oxygen free radicals within neurons. Consequently, this process results in the degeneration of dopaminergic neurons [27]. The 6-OHDA-induced PD model has been widely employed to investigate various aspects of PD pathophysiology, including neuroinflammation, neural activity, striatal metabolic connectivity, and neurogenesis in the context of STN-DBS therapy [28–31]. To accurately evaluate the differential impacts of STN-DBS frequencies, treatment was initiated four weeks post 6-OHDA injection to coincide with the progressive motor impairment observed in the PD model rats.

NSCs in the neurogenic zone (SVZ and SGZ) can self-renew and differentiate into neurons, influenced by molecular signals [32]. Research on PD rats showed a significant drop in proliferating cells in the SVZ, which our investigation links to a decrease in specific cell types (Sox2⁺, GFAP⁺ and DCX⁺ cells) following unilateral 6-OHDA injection [16]. This decline could be attributed to the direct toxicity of 6-OHDA, causing damage to NSCs, or the impact of dopamine neurons in the lesioned striatum through the AT2 receptor [33,34]. Recently, several studies have revealed the regulatory effect of electrical stimulation on neuro-regeneration in the SVZ [35–37]. Our study further establishes that 130Hz STN-DBS boosts NSC proliferation as indicated by increased numbers of BrdU⁺/Sox2⁺ and Ki67⁺/GFAP⁺ cells in the SVZ, underscoring STN-DBS's role in promoting NSC proliferation in both hemispheres. It has been reported that some NSCs extend their foot processes through the ependymal layer, enabling them to receive signals from both the cerebrospinal fluid (CSF) and the bloodstream [38,39]. Consequently, as observed in our prior studies on stroke rats, unilateral injection and electrical stimulation significantly influence the proliferation and differentiation of NSCs not only in the treated hemisphere but also in the opposite hemisphere [40]. It is widely acknowledged that certain neurodegenerative diseases causing neuronal death and degeneration can induce structural plasticity in the brain, leading to its self-reconstruction as a compensatory response to impaired neural circuits. This intrinsic ability of the brain to regenerate itself involves the migration of newly generated neurons to the affected region and is referred to as endogenous regenerative repair [41,42]. In our study, the numbers of new NSCs and neuroblasts had a significant correlation with the outcomes of the rotarod performance test, implying that modulating NSC numbers through electrical stimulation may contribute to functional motor improvements. Our study reveals initial findings on dopamine neuron regeneration, but the actual integration into motor-related neural circuits has not been fully confirmed. We only analyzed a limited number of sections from the SVZ, which might not capture its full complexity. Future research should include a more extensive analysis of the SVZ to better understand its role in motor function. Investigating the effects of longer electrical stimulation on neural circuits and motor recovery is also an important avenue. DBS markedly enhances adenosine release, and activation of thalamic adenosine A1 receptors reduces tremors [43]. Additionally, adenosine influences adult neurogenesis, with adenosine A1 receptor activation stimulating NSC proliferation through the MEK/ERK and Akt pathways [44–46]. The complexity of electrical stimulation's mechanisms necessitates focused future studies to unravel the precise links between electrical stimulation and SVZ neurogenesis.

Neuronal loss in the OB is prevalent in PD, affecting over 95% of patients with significant olfactory impairments [47,48]. In our PD rat model, we observed a significant decrease in the proliferation of NSCs and the production of newly formed neuroblasts in the RMS, a critical pathway for olfactory neuronal networks [49,50]. Remarkably, a week of electrical stimulation notably enhanced NSC and neuroblast presence in the RMS, indicating that STN-DBS could facilitate neurogenesis and potentially ameliorate olfactory deficits in PD patients [51,52]. A limitation of our study is the exclusion of olfactory bulb samples, we focused instead on the SVZ and RMS, which limits a full appreciation of electrical stimulation's impact. Future research will aim to include detailed analysis of the OB to broaden our understanding of electrical stimulation's therapeutic potential for PD.

Electrical stimulation parameters, including contact points, amplitude, frequency, and pulse width, are tailored to clinical needs. Frequency is particularly crucial, influencing intervention effectiveness, with evidence linking it to clinical responses [53]. Research conducted using DTI has demonstrated that electrical stimulation at different frequencies can lead to diverse changes in neural networks. For instance, it has been observed that white matter and fibers are more abundant when using STN-DBS at a frequency of 130 Hz compared to 30 Hz [54]. Additionally, a recent study found that applying a frequency of 60 Hz or higher resulted in a noticeable increase in dopamine concentration following the stimulation [55]. Specifically, we found that stimulation at high frequency (180 Hz) significantly enhanced motor functions and induced a notable increase in Sox2⁺ cell proliferation within the SVZ. In contrast, stimulation at a low frequency (60 Hz) did not lead to marked improvements in either motor function, dopamine synthesis, or the process of neurogenesis. The differential impact of stimulation frequency may be intricately linked to adenosine's role in the brain, underscoring the need for frequency-specific strategies in neural rehabilitation and treatment [56].

The study sheds light on the nuanced effects of STN-DBS frequencies on motor function and neurogenesis which were both impaired in PD model rats. It highlights that a high frequency (130Hz) stimulation not only markedly improves motor deficits and protects dopaminergic neurons but also significantly encourages the proliferation and differentiation of NSCs in the SVZ and RMS, leveraging the potential of the brain's endogenous regenerative repair mechanisms. In stark contrast, low frequency (60Hz) stimulation offers no substantial benefits, underscoring the critical importance of optimizing stimulation frequency for enhancing neurogenesis and motor rehabilitation in PD therapy. This discovery opens new pathways for tailored neurotherapeutic strategies, emphasizing the intricate interplay between electrical stimulation frequency and the brain's inherent capacity for self-repair and functional recovery.

Funding

The study: was supported by grants from Beijing Hospitals Authority Ascent Plan (DFL20190801), Capital Health Research and Development of Special Project (2020-1-2013), National Natural Science Foundation of China (82001374), and The Beijing Municipal Administration of Hospitals Incubating Program (PX2022034).

CRediT authorship contribution statement

Zheng Wu: Conceptualization, Data curation, Investigation, Methodology, Visualization, Writing – original draft. **Zhiwei Ren:** Writing – review & editing, Funding acquisition. **Runshi Gao:** Data curation, Investigation. **Ke Sun:** Conceptualization, Data curation. **Fangling Sun:** Formal analysis, Methodology. **Tingting Liu:** Formal analysis, Methodology. **Songyang Zheng:** Visualization. **Wen Wang:** Conceptualization, Project administration, Resources, Supervision. **Guojun Zhang:** Conceptualization, Funding acquisition, Project administration, Resources, Supervision, Writing – review & editing.

Declaration of competing interest

The authors declare that they have no known competing financial interests or personal relationships that could have appeared to influence the work reported in this paper.

Appendix A. Supplementary data

Supplementary data to this article can be found online at <https://doi.org/10.1016/j.heliyon.2024.e30730>.

References

- [1] J. Benkert, S. Hess, S. Roy, D. Beccano-Kelly, N. Wiederspohn, J. Duda, C. Simons, K. Patil, A. Gaifullina, N. Mannal, E. Dragicevic, D. Spaich, S. Muller, J. Nemeth, H. Hollmann, N. Deuter, Y. Mousba, C. Kubisch, C. Poetschke, J. Striessnig, O. Pongs, T. Schneider, R. Wade-Martins, S. Patel, R. Parlato, T. Frank, P. Kloppenburg, B. Liss, Cav2.3 channels contribute to dopaminergic neuron loss in a model of Parkinson's disease, *Nat. Commun.* 10 (2019) 5094.
- [2] M. Garcia-Garrote, J.A. Parga, P.J. Labandeira, J.L. Labandeira-Garcia, J. Rodriguez-Pallares, Dopamine regulates adult neurogenesis in the ventricular-subventricular zone via dopamine D3 angiotensin type 2 receptor interactions, *Stem Cell.* 39 (2021) 1778–1794.
- [3] B. Shohayeb, M. Diab, M. Ahmed, D. Ng, Factors that influence adult neurogenesis as potential therapy, *Transl. Neurodegener.* 7 (2018) 4.
- [4] V. Murtaj, E. Butti, G. Martino, P. Panina-Bordignon, Endogenous neural stem cells characterization using omics approaches: current knowledge in health and disease, *Front. Cell. Neurosci.* 17 (2023).
- [5] R.C. Sellnow, J.H. Newman, N. Chambers, A.R. West, K. Steece-Collier, I.M. Sandoval, M.J. Benskey, C. Bishop, F.P. Manfredsson, Regulation of dopamine neurotransmission from serotonergic neurons by ectopic expression of the dopamine D2 autoreceptor blocks levodopa-induced dyskinesia, *Acta Neuropathol Commun* 7 (2019) 8.
- [6] K. Rejdak, H. Sienkiewicz Jarosz, P. Bienkowski, A. Alvarez, Modulation of neurotrophic factors in the treatment of dementia, stroke and TBI: effects of Cerebrolysin, *Med. Res. Rev.* 43 (2023) 1668–1700.
- [7] S.A. van den Berge, M.E. van Strien, J.A. Korecka, A.A. Dijkstra, J.A. Sluijs, L. Kooijman, R. Eggers, L. De Filippis, A.L. Vescovi, J. Verhaagen, W.D. van de Berg, E.M. Hol, The proliferative capacity of the subventricular zone is maintained in the parkinsonian brain, *Brain* 134 (2011) 3249–3263.
- [8] V. Donega, S.M. Burm, M.E. van Strien, E.J. van Bodegraven, I. Paliukhovich, H. Geut, W. van de Berg, K.W. Li, A.B. Smit, O. Basak, E.M. Hol, Transcriptome and proteome profiling of neural stem cells from the human subventricular zone in Parkinson's disease, *Acta Neuropathol Commun* 7 (2019) 84.
- [9] G.C. O'Keefe, P. Tyers, D. Aarsland, J.W. Dalley, R.A. Barker, M.A. Caldwell, Dopamine-induced proliferation of adult neural precursor cells in the mammalian subventricular zone is mediated through EGF, *Proc Natl Acad Sci U S A.* 106 (2009) 8754–8759.

- [10] N. Freundlieb, C. Francois, D. Tande, W.H. Oertel, E.C. Hirsch, G.U. Hoglinger, Dopaminergic substantia nigra neurons project topographically organized to the subventricular zone and stimulate precursor cell proliferation in aged primates, *J. Neurosci.* 26 (2006) 2321–2325.
- [11] P.M. Aponso, R.L. Faull, B. Connor, Increased progenitor cell proliferation and astrogenesis in the partial progressive 6-hydroxydopamine model of Parkinson's disease, *Neuroscience* 151 (2008) 1142–1153.
- [12] H.M. Khoo, H. Kishima, K. Hosomi, T. Maruo, N. Tani, S. Oshino, T. Shimokawa, M. Yokoe, H. Mochizuki, Y. Saitoh, T. Yoshimine, Low-frequency subthalamic nucleus stimulation in Parkinson's disease: a randomized clinical trial, *Movement Disorders* 29 (2014) 270–274.
- [13] V. Ricchi, M. Zibetti, S. Angrisano, A. Merola, N. Arduino, C.A. Artusi, M. Rizzzone, L. Lopiano, M. Lanotte, Transient effects of 80 Hz stimulation on gait in STN DBS treated PD patients: a 15 months follow-up study, *Brain Stimul.* 5 (2012) 388–392.
- [14] C. Sidiropoulos, Low-frequency stimulation of STN-DBS reduces aspiration and freezing of gait in patients with PD, *Neurology* 85 (2015) 557.
- [15] V. Vedam-Mai, B. Gardner, M.S. Okun, F.A. Siebzehrubel, M. Kam, P. Aponso, D.A. Steindler, A.T. Yachnis, D. Neal, B.U. Oliver, S.J. Rath, R.L.M. Faull, B. A. Reynolds, M.A. Curtis, Increased precursor cell proliferation after deep brain stimulation for Parkinson's disease: a human study, *PLoS One* 9 (2014) e88770.
- [16] V. Khaindrava, P. Salin, C. Melon, M. Ugrumov, L. Kerkerian-Le-Goff, A. Daszuta, High frequency stimulation of the subthalamic nucleus impacts adult neurogenesis in a rat model of Parkinson's disease, *Neurobiol. Dis.* 42 (2011) 284–291.
- [17] L. He, Z. Sun, J. Li, R. Zhu, B. Niu, K.L. Tam, Q. Xiao, J. Li, W. Wang, C.Y. Tsui, L.V. Hong, K.F. So, Y. Xu, S. Ramakrishna, Q. Zhou, K. Chiu, Electrical stimulation at nasocale topography boosts neural stem cell neurogenesis through the enhancement of autophagy signaling, *Biomaterials* 268 (2021) 120585.
- [18] S.J. Park, J.S. Park, H.N. Yang, S.W. Yi, C. Kim, K. Park, Neurogenesis is induced by electrical stimulation of human Mesenchymal stem cells Co-cultured with mature neuronal cells, *Macromol. Biosci.* 15 (2015) 1586–1594.
- [19] R. Zhu, Z. Sun, C. Li, S. Ramakrishna, K. Chiu, L. He, Electrical stimulation affects neural stem cell fate and function in vitro, *Exp. Neurol.* 319 (2019) 112963.
- [20] M. Muthuraman, M. Palotai, B. Javor-Duray, A. Kelemen, N. Koirala, L. Halasz, L. Eross, G. Fekete, L. Bognar, G. Deuschl, G. Tamas, Frequency-specific network activity predicts bradykinesia severity in Parkinson's disease, *Neuroimage Clin* 32 (2021) 102857.
- [21] J.N. Strelow, T.A. Dembek, J.C. Baldermann, P. Andrade, G.R. Fink, V. Visser-Vandewalle, M.T. Barbe, Low beta-band suppression as a tool for DBS contact selection for akinetic-rigid symptoms in Parkinson's disease, *Parkinsonism Relat. Disorders* 112 (2023) 105478.
- [22] T. Yamamoto, T. Uchiyama, R. Sakakibara, J. Taniguchi, S. Kuwabara, The subthalamic activity and striatal monoamine are modulated by subthalamic stimulation, *Neuroscience* 259 (2014) 43–52.
- [23] C. Anderson, D. Sheppard, A.D. Dorval, Parkinsonism and subthalamic deep brain stimulation dysregulate behavioral motivation in a rodent model, *Brain Res.* 1736 (2020) 146776.
- [24] Y.C. Chang, W.Y. Li, L.J. Lee, L.J. Lee, Interplay of Prenatal and Postnatal Risk factors in the behavioral and histological features of a "Two-Hit" non-genetic mouse model of schizophrenia, *Int. J. Mol. Sci.* 21 (2020).
- [25] Y.L. Huang, N.X. Zeng, J. Chen, J. Niu, W.L. Luo, P. Liu, C. Yan, L.L. Wu, Dynamic changes of behaviors, dentate gyrus neurogenesis and hippocampal miR-124 expression in rats with depression induced by chronic unpredictable mild stress, *Neural Regen Res* 15 (2020) 1150–1159.
- [26] X. Liu, H. Ren, A. Peng, H. Cheng, J. Chen, X. Xia, T. Liu, X. Wang, The effect of RADA16-I and CDNF on neurogenesis and neuroprotection in brain ischemia-reperfusion injury, *Int. J. Mol. Sci.* 23 (2022).
- [27] A. Schober, Classic toxin-induced animal models of Parkinson's disease: 6-OHDA and MPTP, *Cell Tissue Res.* 318 (2004) 215–224.
- [28] N. Apetz, E. Kordys, M. Simon, B. Mang, M. Aswendt, D. Wiedermann, B. Neumaier, A. Drzezga, L. Timmermann, H. Endeppols, Effects of subthalamic deep brain stimulation on striatal metabolic connectivity in a rat hemiparkinsonian model, *Dis Model Mech* 12 (2019).
- [29] Y. Chen, G. Zhu, D. Liu, X. Zhang, Y. Liu, T. Yuan, T. Du, J. Zhang, Subthalamic nucleus deep brain stimulation suppresses neuroinflammation by Fractalkine pathway in Parkinson's disease rat model, *Brain Behav. Immun.* 90 (2020) 16–25.
- [30] A. Nasrolahi, J. Mahmoudi, M. Karimpour, A. Akbarzadeh, S. Sadigh-Eteghad, R. Salehi, F. Farajdokht, M. Farhoudi, Effect of cerebral dopamine neurotrophic factor on endogenous neural progenitor cell migration in a rat model of Parkinson's disease, *EXCLI J* 18 (2019) 139–153.
- [31] C. Yu, I.R. Cassar, J. Sambangi, W.M. Grill, Frequency-specific optogenetic deep brain stimulation of subthalamic nucleus improves parkinsonian motor behaviors, *J. Neurosci.* 40 (2020) 4323–4334.
- [32] M. Götz, M. Nakafuku, D. Petrik, Neurogenesis in the developing and adult brain—similarities and key differences, *Cold Spring Harbor Perspect. Biol.* 8 (2016) a018853.
- [33] J.E. Lee, Y.J. Shin, Y.S. Kim, H.N. Kim, D.Y. Kim, S.J. Chung, H.S. Yoo, J.Y. Shin, P.H. Lee, Uric acid enhances neurogenesis in a parkinsonian model by remodeling mitochondria, *Front. Aging Neurosci.* 14 (2022).
- [34] A. Mishra, S. Singh, V. Tiwari, S. Bano, S. Shukla, Dopamine D1 receptor agonism induces dynamin related protein-1 inhibition to improve mitochondrial biogenesis and dopaminergic neurogenesis in rat model of Parkinson's disease, *Behav. Brain Res.* 378 (2020) 112304.
- [35] H.H. Liu, Y. Xiang, T.B. Yan, Z.M. Tan, S.H. Li, X.K. He, Functional electrical stimulation increases neural stem/progenitor cell proliferation and neurogenesis in the subventricular zone of rats with stroke, *Chin Med J (Engl)*. 126 (2013) 2361–2367.
- [36] Q. Liu, Y. Jiao, W. Yang, B. Gao, D.K. Hsu, J. Nolte, M. Russell, B. Lyeth, T.P. Zanto, M. Zhao, Intracranial alternating current stimulation facilitates neurogenesis in a mouse model of Alzheimer's disease, *Alzheimer's Res. Ther.* 12 (2020) 89.
- [37] Z. Wu, F. Sun, Z. Li, M. Liu, X. Tian, D. Guo, P. Wei, Y. Shan, T. Liu, M. Guo, Z. Zhu, W. Zheng, Y. Wang, G. Zhao, W. Wang, Electrical stimulation of the lateral cerebellar nucleus promotes neurogenesis in rats after motor cortical ischemia, *Sci. Rep.* 10 (2020) 16563.
- [38] Y. Dillen, H. Kemps, P. Gervois, E. Wolfs, A. Bronckaers, Adult neurogenesis in the subventricular zone and its regulation after ischemic stroke: implications for therapeutic approaches, *Transl Stroke Res* 11 (2020) 60–79.
- [39] M. Jiang, S.E. Jang, L. Zeng, The effects of extrinsic and intrinsic factors on neurogenesis, *Cells* 12 (2023) 1285.
- [40] Z. Wu, F. Sun, Z. Li, M. Liu, X. Tian, D. Guo, P. Wei, Y. Shan, T. Liu, M. Guo, Z. Zhu, W. Zheng, Y. Wang, G. Zhao, W. Wang, Electrical stimulation of the lateral cerebellar nucleus promotes neurogenesis in rats after motor cortical ischemia, *Sci. Rep.* 10 (2020) 16563.
- [41] Z. Liu, Z. Wang, Z. Zhu, J. Hong, L. Cui, Y. Hao, G. Cheng, R. Tan, Crocetin regulates functions of neural stem cells to generate new neurons for cerebral ischemia recovery, *Adv. Healthcare Mater.* 12 (2023) e2203132.
- [42] L. Zhang, J. Zhang, X. Zhu, W. Jiao, Y. Yang, Y. Wu, L. Yang, Y. Wang, Metformin enhances neural precursor cells migration and functional recovery after ischemic stroke in mice, *Exp. Brain Res.* 241 (2023) 505–515.
- [43] L. Bekar, W. Libionka, G. Tian, Q. Xu, A. Torres, X. Wang, D. Lovatt, E. Williams, T. Takano, J. Schnerrmann, R. Bakos, M. Nedergaard, Adenosine is crucial for deep brain stimulation-mediated attenuation of tremor, *Nat. Med.* 14 (2008) 75–80.
- [44] H. Gao, X. Cheng, J. Chen, C. Ji, H. Guo, W. Qu, X. Dong, Y. Chen, L. Ma, Q. Shu, X. Li, Fto-modulated lipid niche regulates adult neurogenesis through modulating adenosine metabolism, *Hum. Mol. Genet.* 29 (2020) 2775–2787.
- [45] H. Migita, K. Kominami, M. Higashida, R. Maruyama, N. Tuchida, F. McDonald, F. Shimada, K. Sakurada, Activation of adenosine A1 receptor-induced neural stem cell proliferation via MEK/ERK and Akt signaling pathways, *J. Neurosci. Res.* 86 (2008) 2820–2828.
- [46] T.C.B. Piermartiri, B. Dos Santos, F.G.Q. Barros-Aragão, R.D. Prediger, C.I. Tasca, Guanosine promotes proliferation in neural stem cells from Hippocampus and neurogenesis in adult mice, *Mol. Neurobiol.* 57 (2020) 3814–3826.
- [47] A. Haehner, T. Hummel, H. Reichmann, Olfactory Loss in Parkinson's Disease, vol. 2011, *Parkinsons Dis*, 2011 450939.
- [48] H.S. Rethinavel, S. Ravichandran, R.K. Radhakrishnan, M. Kandasamy, COVID-19 and Parkinson's disease: defects in neurogenesis as the potential cause of olfactory system impairments and anosmia, *J. Chem. Neuroanat.* 115 (2021) 101965.
- [49] T. Fuchigami, Y. Itokazu, J.C. Morgan, R.K. Yu, Restoration of adult neurogenesis by intranasal administration of gangliosides GD3 and GM1 in the olfactory bulb of A53T alpha-synuclein-expressing Parkinson's-disease model mice, *Mol. Neurobiol.* 60 (2023) 3329–3344.
- [50] N. Genet, G. Genet, N.W. Chavkin, U. Paila, J.S. Fang, H.H. Vasavada, J.S. Goldberg, B.R. Acharya, N.S. Bhatt, K. Baker, S.P. McDonnell, M. Huba, D. Sankaranarayanan, G.Z.M. Ma, A. Eichmann, J. Thomas, C. French-Constant, K.K. Hirschi, Connexin 43-mediated neurovascular interactions regulate neurogenesis in the adult brain subventricular zone, *Cell Rep.* 42 (2023) 112371.

- [51] C. Li, Y. Hou, X. Wang, Y. Li, F. Li, C. Zhang, W. Li, Impact of subthalamic deep brain stimulation on hyposmia in patients with Parkinson's disease is influenced by constipation and dysbiosis of microbiota, *Front. Neurol.* 12 (2021).
- [52] O. Saatci, N.H. Yilmaz, A. Zirh, B. Yulug, The therapeutic effect of deep brain stimulation on olfactory functions and clinical scores in Parkinson's disease, *J. Clin. Neurosci.* 68 (2019) 55–61.
- [53] V. Dayal, P. Limousin, T. Foltynie, Subthalamic nucleus deep brain stimulation in Parkinson's disease: the effect of varying stimulation parameters, *J. Parkinsons Dis.* 7 (2017) 235–245.
- [54] Z. Li, Y. Guo, X. Bao, J. Lei, Z. Shen, X. Wang, L. Li, Y. Li, R. Wang, Effects of subthalamic deep brain stimulation with different frequencies in a parkinsonian rat model, *Neuromodulation: Technology at the Neural Interface* 24 (2021) 220–228.
- [55] G. Xiao, Y. Song, Y. Zhang, Y. Xing, S. Xu, M. Wang, J. Wang, D. Chen, J. Chen, X. Cai, Dopamine and striatal neuron firing respond to frequency-dependent DBS detected by microelectrode arrays in the rat model of Parkinson's disease, *Biosensors* 10 (2020) 136.
- [56] S.P. Perrier, M. Gleizes, C. Fonta, L.G. Nowak, Effect of adenosine on short-term synaptic plasticity in mouse piriform cortex in vitro: adenosine acts as a high-pass filter, *Phys. Rep.* 7 (2019) e13992.